

MODELLING OF A WASTE ROCK DUMP DESIGN TO CONTROL ACID ROCK DRAINAGE AT THE SVARTLIDEN GOLD MINE, NORTHERN SWEDEN¹

Claire M.Linklater², John W. Bennett, and Neale Edwards

Abstract. The Svartliden Gold Project has developed a complex design for waste rock dumps on the site. The design proposes encapsulation of potentially acid-forming material as cells within un-reactive material. Acid-forming material will be categorised as high risk or low risk, and within the overall dump design, cells involving high risk material will include a lining comprising low permeability glacial till. Acid generation is to be controlled by inhibiting contact between the reactive materials and oxygen, which must be supplied via diffusion of gas from the outer dump surfaces to the interior of the cells. Construction of such a complex dump is non-trivial and careful consideration has been given to the predicted long-term performance of the proposed strategy.

This paper describes how modelling techniques have been applied to quantify the benefits of the more complex dump design when compared with alternative simpler designs. The long-term performance of the dump was modelled using SULFIDOX. SULFIDOX takes a two-dimensional representation of the dump, and simulates the temporal and spatial evolution of key chemical and physical processes, e.g. diffusion and advection of gaseous components, infiltration of water, mineral reactions, heat conduction. For this work, an improved version of SULFIDOX was used that extends the approach so that heterogeneity in the initial dump configuration can be represented, allowing cells and other structures within the dump to be modelled.

Using SULFIDOX, it was possible to quantify benefits that the proposed dump design for the Svartliden site would deliver, namely (i) a significant reduction in the magnitude of any short-term peaks in contaminant load and (ii) management of the load profile so that contaminant levels remain below certain thresholds throughout the lifetime of the dump.

Additional key words: sulfides, oxidation

¹ Paper presented at the 7th International Conference on Acid Rock Drainage (ICARD), March 26-30, 2006, St. Louis MO. R.I. Barnhisel (ed.) Published by the American Society of Mining and Reclamation (ASMR), 3134 Montavesta Road, Lexington, KY 40502

² Claire M. Linklater is a senior geochemist with ANSTO Minerals, PMB 1, Menai, NSW 2234, Australia. John W. Bennett is a Senior Principal Research Scientist with ANSTO Minerals. Neale Edwards is the Chief Geologist for Dragon Mining NL, PO Box 8048, Perth BC, WA 6849, Australia.

7th International Conference on Acid Rock Drainage, 2006 pp 1079-1105

DOI: 10.21000/JASMR06021079

<https://doi.org/10.21000/JASMR06021079>

Introduction

The Svartliden Gold Project is located in northern Sweden, see Fig. 1. The mine came into production in March 2005 and is the first integrated mine and treatment plant to be developed under the new Swedish Environment and Mining Acts.

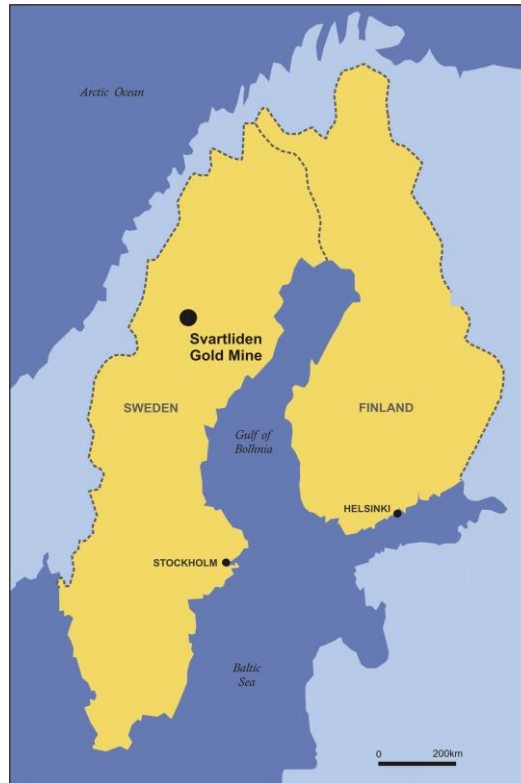


Figure 1. Map showing locations of Dragon Mining projects around the world. The Svartliden Gold Project is located in northern Sweden.

The Svartliden gold (Au) deposit is a greenfields discovery situated on the far southwest margin of the Skellefte District, in an area that is rapidly developing into a new gold-rich mineral province. It represents a style of mineralisation previously not found in the District – epigenetic Au and Ag in hydrothermally altered ductile shear zones, hosted within early Proterozoic volcanics and sediments, which have been metamorphosed to a mid-amphibolite grade facies.

The ore is being mined as a single open pit feeding an adjacent leach treatment plant. When fully operational, it is anticipated that the mine will produce 50,000 to 60,000 ounces of Au per annum.

Over the lifetime of the mine, more than 4 million cubic metres of waste rock will be produced, over 13 per cent of which could contain sulfides. Detailed characterisation of mine waste materials (Comarmond et al., 2003; Brown and Comarmond, 2002, 2003) has led to the following classification scheme:

- High risk potentially acid forming (PAF);

- Low capacity potentially acid forming (LC PAF);
- Non acid forming (NAF).

These wastes must be managed so that potential acid generation can be controlled and the environmental risks minimised. A number of management options exist. For example, different waste types can be disposed of in separate dumps or together as part of a composite dump design. The strategy adopted will not alter the volume of wastes to be managed and often the selection of an appropriate dump design(s) must encompass consideration of available ground and mine scheduling. The proposed dump design at Svartliden involves encapsulation of potentially acid-forming materials as cells within un-reactive material. Cells involving high risk material will include a lining comprising low-permeability glacial till. The design principle is that acid generation is controlled by inhibiting contact between the reactive materials and O₂, which must be supplied via transport of gas from the outer dump surfaces to the interior of the cells.

Figure 2 shows a plan view of the proposed Svartliden dump design. Construction of such a complex dump is non-trivial and careful consideration has been given to the predicted long-term performance of the dump. To build confidence in the benefits of this complex waste rock dump design as opposed to simpler alternatives, the modelling code SULFIDOX has been used to predict the long-term evolution of different dump designs.

Methods

Description of the SULFIDOX model

SULFIDOX implements a conceptual model of oxidation and transport processes in sulfidic waste rock dumps (Pantelis et al., 2002), along with a detailed model of chemical interactions within the dumps. In summary, SULFIDOX describes a three phase system consisting of a rigid solid porous phase through which flow gas and water phases. The following processes can be represented:

- Gas transport via diffusion and advection. Diffusive gas transport is driven by O₂ concentration gradients caused by the consumption of O₂ by reaction within the dump. Advective gas transport is driven by pressure or density gradients, for example, caused by temperature gradients that form as a consequence of heat released by reactions in the dump;
- Heat transport via thermal conduction and advective fluid flow. Two fluids are involved in the advective transport, the liquid infiltrating the dump and gas flowing through the dump;
- Infiltration of water down through the waste rock dump. A constant infiltration rate is maintained at the dump surface (the top and the batters) for the entire duration of the simulation. Water content distribution over the entire dump is represented by a steady state approximation that incorporates the physical properties of the waste rock material and the applied infiltration flux. Water flow is uniform, as described by Richard's Equation. Water discharges evenly across the base of the heap at the same rate at which it infiltrates the heap surface;
- Transport of water-borne components via diffusion and advection in the liquid phase;

- Speciation and complexation of chemical components within the water. Usually based on thermodynamic equilibrium laws, incorporated by the inclusion of a modular geochemical speciation code based on HARPHRQ (Brown et al., 1991), a modified version of PHREEQE (Parkhurst et al., 1980). Kinetically controlled interactions (e.g. conversion of Fe^{+2} to Fe^{+3}) can also be represented;
- Dissolution of minerals in the dump; both slow dissolution subject to kinetic controls, and rapid ‘instantaneous’ dissolution subject to thermodynamic equilibrium laws;
- Precipitation of secondary minerals within the dump (based on thermodynamic equilibrium laws).

Within SULFIDOX, a two-dimensional cross-section of the dump is assumed to approximate a trapezoidal geometry, within which a computational grid is defined. Transport of heat, gas, and water between grid points is computed based on fundamental physics principles (such as the heat equation and Richard’s Equation). Finite difference methodology is used. Full descriptions of the numerical methods adopted in the code are given in Brown et al, 2001.

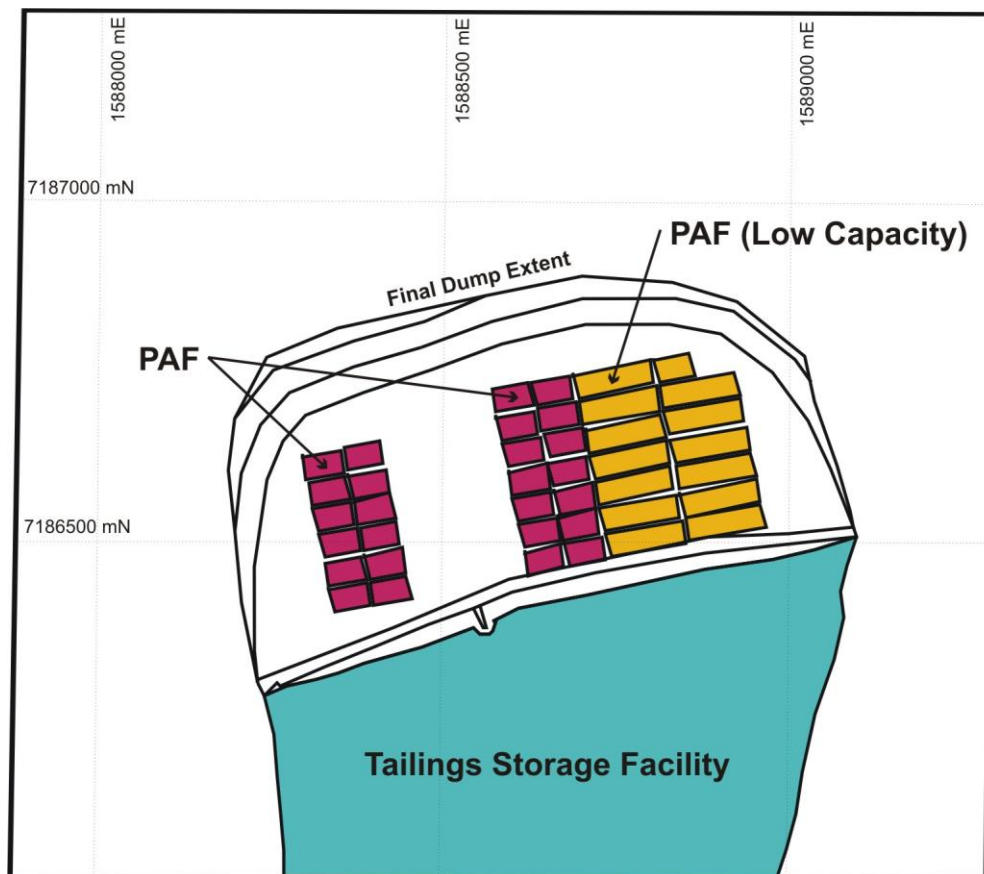


Figure 2. Plan view of the Svartliden dump design.

The standard version of SULFIDOX assumes that, at the start of a simulation, the chemical and physical properties of the dump are homogeneous. The new version of the code allows representation of spatial variability within the initial dump configuration, e.g. ‘cells’ and/or ‘layers’ of material with distinct properties.

Parameterisation of the SULFIDOX model

Initialisation of the SULFIDOX model requires that values be assigned to a range of system parameters:

- site-specific parameters – e.g. ambient temperature, average annual rainfall, altitude;
- dump-specific parameters – e.g. dimensions, batter angles, quantities and positioning of different materials, physical and chemical properties of the materials;
- generic physical constants – e.g. values are required for viscosity, heat conductivity, etc, for different phases present in the dump (solid, liquid, gas);
- parameters to characterise chemical and physical processes included in the model – e.g. reaction stoichiometry, kinetic rate expressions, dump water content (as a control of gas diffusivity).

As far as possible, site- and dump-specific parameter values were selected based on available measured data from the Svartliden site. Where measured data showed variability, average values were selected. Where data were unavailable, suitable parameter values were estimated based on information derived from studies of other waste rock dumps. Generic physical constants and other parameters were sourced from relevant published data sources.

Some key parameter values used in the current study are given in Tables 1 and 2. As indicated, some of these parameter values are subject to significant uncertainty. In these cases sensitivity calculations have been undertaken to determine the impact that these uncertainties might have on model outputs. The results of these sensitivity calculations are described later in this paper.

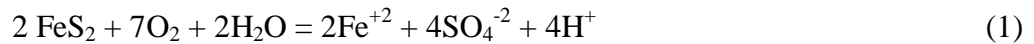
Table 1. Site-specific input parameters used in the SULFIDOX calculations

Parameter	Value	Comment
Atmospheric oxygen concentration	20.95 vol%	
Altitude	460 m	
Initial temperature within the waste rock dump	1°C	Average seasonal temperatures at the site range from – 12.9 to +14.5. The selected value lies at the mid-point of this range. SULFIDOX assumes that, initially, the temperature within the dump is homogeneous. During the simulation, the temperature within the dump varies spatially and temporally due to the progress of exothermic sulfide oxidation.
Water infiltration rate	0.446 m yr ⁻¹	This is an estimated value based on the difference between the annual precipitation (692 mm) and annual evaporation (246 mm). The value is subject to considerable uncertainty due to (i) seasonal variability in precipitation and evaporation data, (ii) the fact that run-off has not been accounted for.
Composition of the infiltrating water	pH 4.9 6.3×10 ⁻⁶ M H ₂ SO ₄	Slightly acidic water, to approximate weakly acidic rain.

Table 2. Properties of the different waste materials in the modelled dumps

	High risk PAF	Low Capacity PAF	NAF (granite)	Glacial Till	Comment
Gas permeability, m ²	10 ⁻¹⁰			10 ⁻¹⁴	For the PAF, LC PAF and NAF materials this property is not known, and may vary spatially. Values for typical dump materials range from 10 ⁻¹³ to 10 ⁻¹⁰ m ² (Ritchie, 1994). For PAF, LC PAF and NAF a reasonable intermediate value was selected. The hydraulic conductivity of the glacial till has been measured, 1.3 x 10 ⁻⁷ m s ⁻¹ . Based on this value, the air permeability can be calculated using the expression: $K_g = \frac{K_s \mu_w}{\rho_w g}$ where K_g is the intrinsic permeability, K_s is the saturated hydraulic conductivity, μ_w is the viscosity of water, ρ_w is the density of water and g the gravitational acceleration.
Porosity	0.29			0.20	Estimates of dump porosity were derived from a comparison of the intrinsic and bulk densities of the materials.
Liquid volume fraction	0.09			0.15	This property was not known. Initial estimates were made based on experience from other waste rock dumps. It was considered that the glacial till, due to fine grain-size and clay-rich properties, would contain a higher fraction of water.
Intrinsic density, kg m ⁻³	3080	3080	2790	2750	Based on measurements undertaken at the site.
IOR, kg(O ₂) m ⁻³ s ⁻¹ [20°C]	1.5×10 ⁻⁷	5×10 ⁻⁸	1.0×10 ⁻⁸	10 ⁻¹²	These values were selected based on previous laboratory studies of the materials (Brown and Comarmond, 2003). The glacial till was considered to be a non-oxidising material and given an arbitrarily low IOR value.
Pyrite content, wt%	1.9	0.6	0.09	0.09	These values were based on previous characterisation studies undertaken on similar samples (Brown and Comarmond, 2003).

Details of the sulfide oxidation model. The model was based on the premise that the main sulfide present in each material was pyrite, FeS₂. In all modelling calculations, the stoichiometry of the pyrite oxidation reaction was as follows:



The reaction is exothermic, being associated with an enthalpy of $2.8 \times 10^6 \text{ J mol}(\text{reaction})^{-1}$. The rate of the reaction is dependent on a number of system parameters e.g. the mass of sulfide present, the availability of O₂ and the catalytic influence of bacteria e.g. Ritchie (1994). In the current work, the oxidation of pyrite was described using the following Monod-type expression:

$$R = S_{\max} \left(\frac{\omega_s}{\Omega_s} \frac{\sigma_1 + 1}{\sigma_1 + \omega_s/\Omega_s} \right) \left(\frac{\omega_O}{\Omega_O} \frac{\sigma_2 + 1}{\sigma_2 + \omega_O/\Omega_O} \right) \quad (2)$$

where:

- R is the reaction rate, kg(S) m⁻³ s⁻¹;
- S_{max} is the maximum reaction rate for the system under ambient conditions of temperature, sulfide and oxygen availability;
- σ₁ and σ₂ are empirical constants;
- Ω_O and Ω_S are the initial O₂ (corresponding to the O₂ mass fraction in the atmosphere at mean ambient conditions) and S mass fractions, respectively; and
- ω_O and ω_S are the current oxygen and sulfide mass fractions, respectively.

Note that Equation 2 does not include any temperature-dependence. Temperature dependence can include an Arrhenius effect (an increase in reaction rate as temperature increases) and also a temperature function related to the bacterial populations that are catalysing the oxidation reaction (bacteria can diminish and die if temperatures are too high). To keep the current calculations as simple as possible, it was decided to exclude temperature dependence from the modelling. Such a simplification was justified because:

- Activation energies measured in the field are typically low. Activation energy, E_a, is an important input to the Arrhenius relationship. Values for E_a measured in the laboratory range up to 80 kJ mol⁻¹ (Nicholson, 1994) (which would equate to an increase in reaction rate of around a factor of two for every 5°C in temperature). However, temperature dependence observed in the field is often minimal (Bennett et al., 1993) and appropriate E_a values are considered to be 20 kJ mol⁻¹ or less. These low E_a values would correspond to an increase in reaction rate of less than 20 per cent for every 5°C.
- Temperatures will not reach high enough values to affect bacteria populations. Temperatures at the site are relatively low (maximum temperature reached is <15°C), and preliminary simulations indicated that heating due to oxidation was limited to a few degrees only. Temperatures are therefore not expected to rise to values where bacterial activity is inhibited (usually considered to be ~40°C).

Data used to parameterise the sulfide oxidation model are summarised in Table 3.

Table 3. Values used to parameterise the sulfide oxidation model

Parameter	Value	Comment										
S_{\max}	<table border="1"> <tr> <td></td> <td>Units: $\text{kg(S)m}^{-3}\text{s}^{-1}$</td> </tr> <tr> <td>PAF</td> <td>8.6×10^{-8}</td> </tr> <tr> <td>LC PAF</td> <td>2.9×10^{-8}</td> </tr> <tr> <td>NAF</td> <td>5.7×10^{-9}</td> </tr> <tr> <td>Till</td> <td>5.7×10^{-13}</td> </tr> </table>		Units: $\text{kg(S)m}^{-3}\text{s}^{-1}$	PAF	8.6×10^{-8}	LC PAF	2.9×10^{-8}	NAF	5.7×10^{-9}	Till	5.7×10^{-13}	These values were calculated based on the IOR values given in Table 2, derived in the laboratory at 20°C. As activation energies are not available for these samples, it was decided not to scale these values down to the lower temperatures relevant for site conditions (Table 1). It is acknowledged therefore that the reaction rates used may be overestimates. This is, however, a conservative approach as SO_4^{-2} loads are likely to be overestimated.
	Units: $\text{kg(S)m}^{-3}\text{s}^{-1}$											
PAF	8.6×10^{-8}											
LC PAF	2.9×10^{-8}											
NAF	5.7×10^{-9}											
Till	5.7×10^{-13}											
σ_1	1.15	This value approximates a power-law with an exponent of $2/3$ and is consistent with a simple ‘shrinking core’ model (Ritchie, 1994; Brown et al., 2001). The initial grain-size of the reacting material is not addressed explicitly by the model. The selected S_{\max} values are believed appropriate measures of reaction rates at early times while system behaviour is dominated by fine particle size material, Bennett et al (2000).										
σ_2	0.05	To approximate a step function, thought to represent more accurately the dependence of bacterially-catalysed reaction rates (for pyritic mine waste) on O_2 concentration (Hammack and Watzlaf, 1990).										

Other model details. To model thermodynamically-controlled reactions (e.g. precipitation of secondary minerals, speciation/complexation of aqueous components) or complex kinetically controlled reactions (e.g. dissolution of aluminosilicates) it is necessary to activate the geochemical module in SULFIDOX, resulting in significantly longer computation times.

As considerable insights to dump behaviour can be gained using a relatively simple geochemical model (considering only the dissolution of sulfide), for the current work it was decided to exclude full geochemistry from the calculations. Output from this simple model includes Fe, H, and SO_4^{-2} levels in water leaving the dump base. This output can be used to assess acidity and contaminant load in dump effluent.

Modeling Approach

The approach adopted was to consider a number of different dump designs. Three cases were defined:

- Case 1:** A dump comprising low capacity PAF material.
- Case 2:** A dump comprising high risk PAF material (with and without a cover comprising low-permeability glacial till).
- Case 3:** A composite dump containing cells of reactive material encapsulated in non-reactive material.

Cases 1 and 2 were included to illustrate how the materials might behave if simply placed in individual dumps on the site. The final, more complex, simulation (Case 3) was undertaken using a dump configuration as close to the proposed Svartliden dump design as possible (within the constraints of existing SULFIDOX capabilities and model run times).

All the simulations involved idealised dump configurations (Fig. 3). The dump dimensions used are summarised in Table 4. The models are based on two-dimensional ‘slices’ through these idealised dump configurations. In order to compare the different model outputs, with each other and with the planned dump, it is necessary to scale the outputs to be representative of a three-dimensional dump. Each modelled ‘slice’ is considered to be 1m in width and equates to a particular volume of material (Table 4). If it can be assumed that there are no significant changes in dump behaviour along the third dimension (reasonable in the case of dumps that are long in the third dimension) then a three-dimensional dump can be considered to be a composite of many identical two-dimensional slices. Table 4 includes a value for the ‘length of the dump’. This value corresponds to the length required in the third dimension so that the volume of LC PAF or PAF in the modelled dump equates to the volume to be managed at the Svartliden mine: 297,000m³ and 314,000m³, respectively.

In the Case 3 model, one LC PAF cell is represented and two PAF cells. This configuration differs from the proposed dump design, which involves two LC PAF cells and four PAF cells (Fig. 2). The model uses an idealised configuration in order to reduce the computational times involved in the simulations. Important attributes of the proposed design, e.g. the positioning of the cells 3m above the dump base, are included in the model.

Table 4. Dump dimensions used in the modelling

	Case 1	Case 2	Case 3
Dump height, m	10	10	14
Baselength, m	50	50	500 ¹
Batter angles ²	50°	50°	50°
Volume of modelled 2D trapezoid, m ³	400	400	6804 600 (2×PAF cell ³) 600 (LC PAF ³)
Length of dump (see text for explanation)	785	742.5	500

1. This dimension was selected to be sufficiently wide that the heap batters would not interfere with the region containing the cells. It is not intended to be representative of the width of the planned dump (which may be up to 1km, see Fig. 2).
2. The batter angles determine the spacing of nodes in the SULFIDOX computational domain. For these calculations the batter angle was selected to give a batter gradient ($\Delta x/\Delta y$) of 1.0, allowing equal spacing of nodes in the x and the y direction within the computational grid. The node spacing used in the calculations was 0.2m.
3. The dimensions of the cells were as follows: LC PAF (120m long by 5m high); PAF (60m long by 5m high). Around each PAF cell the till lining is 1m thick.

CASE 1



CASE 2

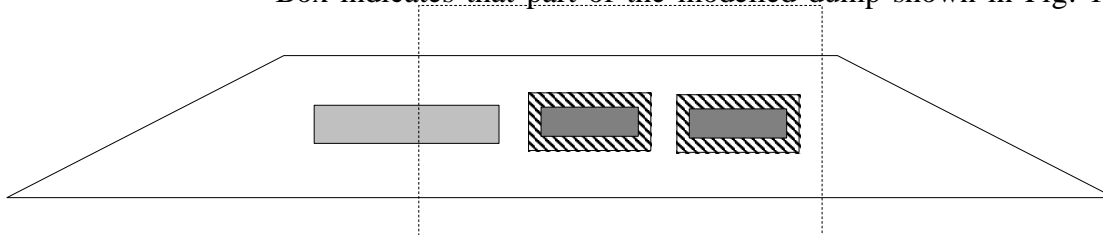


CASE 2 (with a cover)



CASE 3

Box indicates that part of the modelled dump shown in Fig. 10



-  Non-acid forming granite (NAF)
-  Low capacity potential acid-forming (LC PAF)
-  High risk potential acid forming (PAF)
-  Low-permeability glacial till

Figure 3. Schematic diagrams showing the dump configurations used for SULFIDOX simulations. The properties of the different materials are given in Table 2 and dump dimensions are given in Table 4.

Results

Calculated Behaviour for Uncovered Dumps (PAF and LC PAF Material)

Figures 4 and 5 show the calculated spatial distribution of oxygen and pyrite in dumps comprising LC PAF and PAF respectively. Each figure shows outputs at three elapsed times: 1 year, 10 years and 50 years. Both figures show that at 1 and 10 years, there is a large region in the centre of the heap that is depleted with respect to O₂. At these times, sulfide oxidation is confined to the near-surface regions of the dump, where O₂ is available. As oxidation progresses, available pyrite is consumed (as illustrated by the development of zones near the surface that are depleted in pyrite). With time, the oxidation front moves deeper into the dump. In Case 1 (the LC PAF dump) virtually all the pyrite in the dump has been consumed after 50 years. Oxidation (and therefore O₂ consumption) within the dump will be minimal. Under these conditions, oxygen is able to diffuse throughout the dump and concentrations are close to atmospheric values everywhere. In Case 2 (the PAF dump), much more pyrite is present in the dump. Consequently, it takes significantly longer to consume this pyrite and the oxidation front moves more slowly into the dump. At 50 years, remaining pyrite continues to oxidise within the dump.

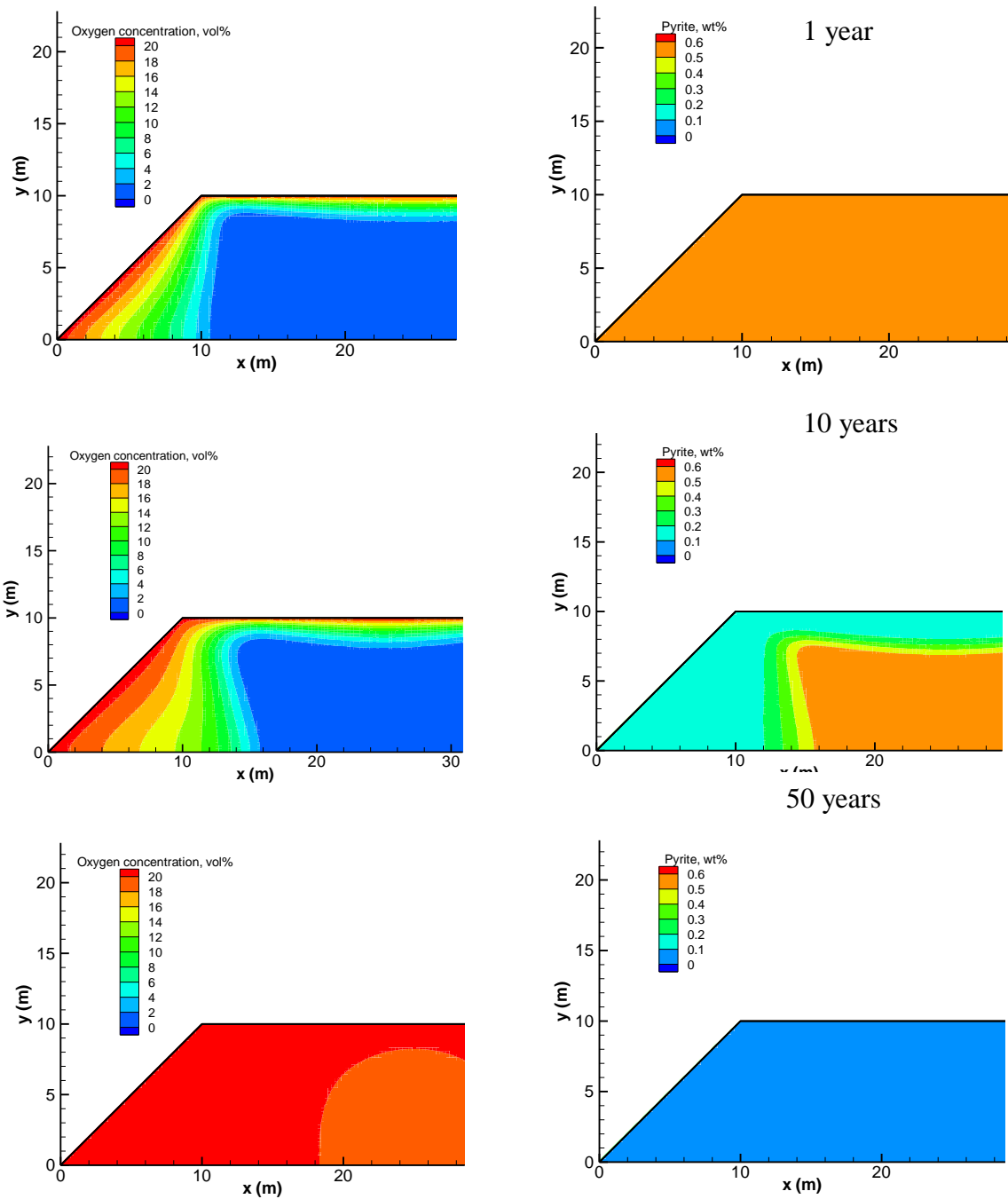


Figure 4. Calculated spatial distribution of oxygen and pyrite, Case 1 (LC PAF dump), at elapsed times of 1 year, 10 years and 50 years.

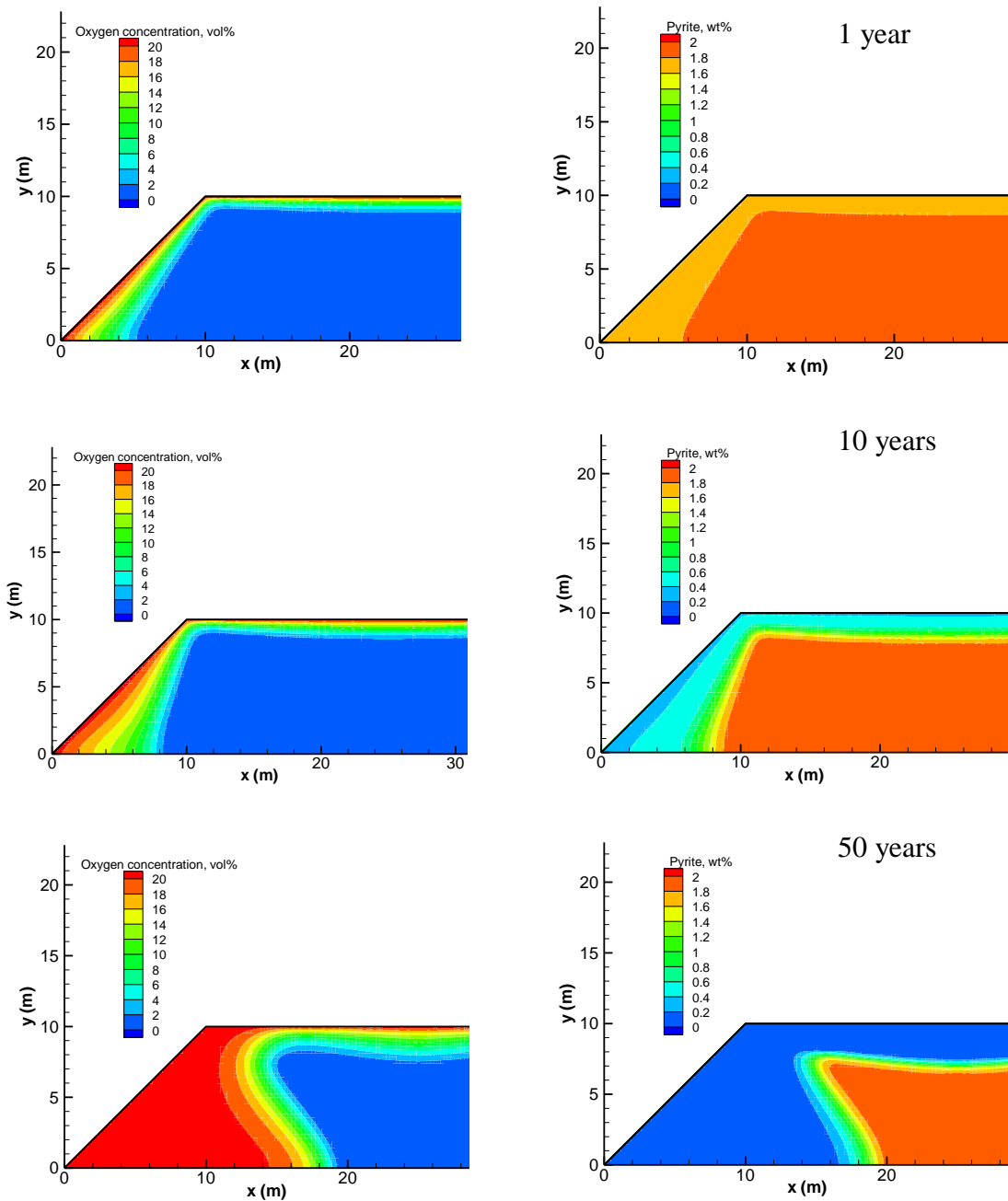


Figure 5. Calculated spatial distribution of oxygen and pyrite, Case 2 (PAF dump) at elapsed time of 1 year, 10 years and 50 years.

Figure 6 shows the temperature distribution after 10 years for both cases, where the initial temperature in the dumps was 1°C. Temperature increases in the dumps due to oxidation were small, less than or equal to 2°C.

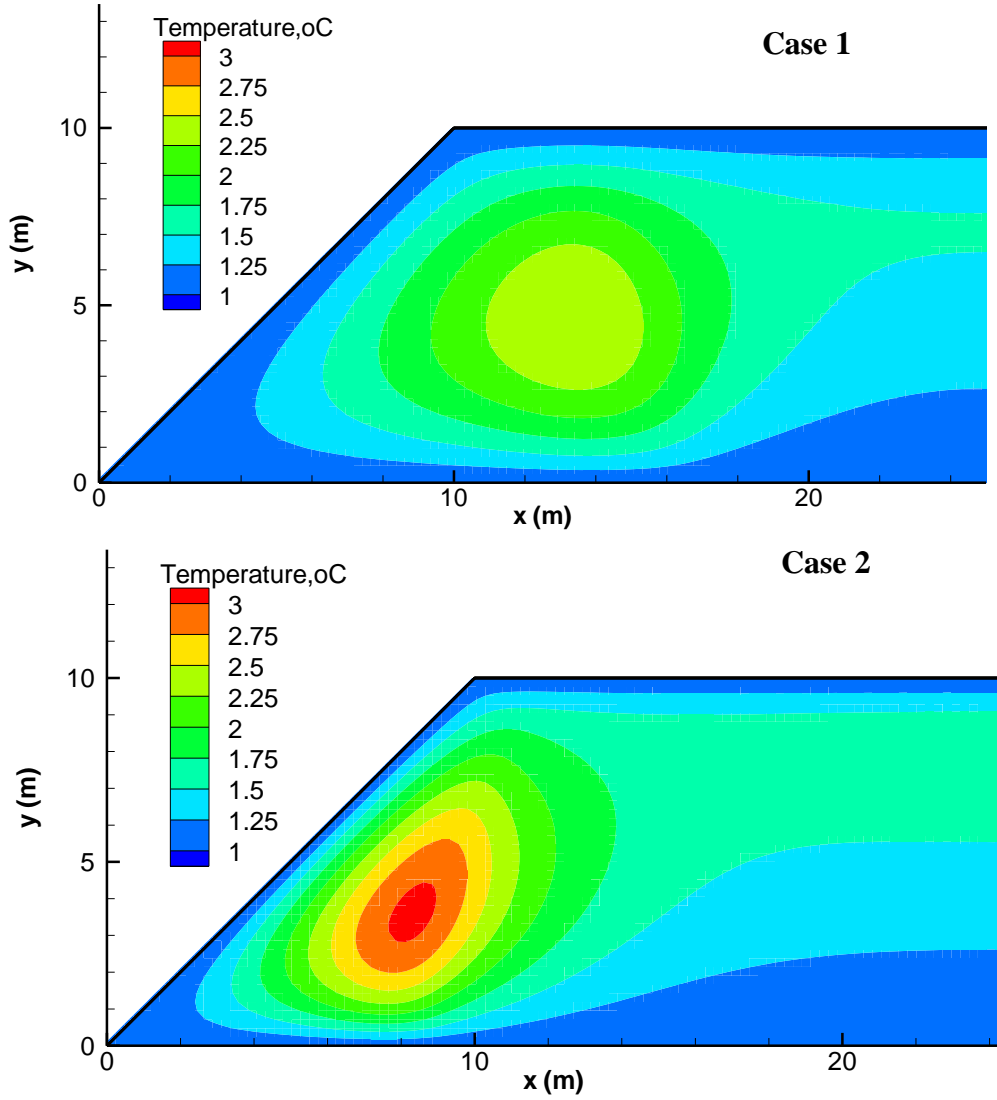


Figure 6. Calculated temperature distribution in Cases 1 and 2 (LC PAF and PAF dumps, respectively) at 10 years.

Figure 7 compares the overall oxidation rates for the two dumps. The calculations predict that the dump comprising PAF will oxidise at a higher overall rate than the dump comprising LC PAF. After 50 years, the overall oxidation rate of the LC PAF dump (Case 1) drops to zero as all the pyrite has been consumed. The PAF dump (Case 2), mainly due to its higher sulfide content, continues to oxidise at about 30% of its maximum value.

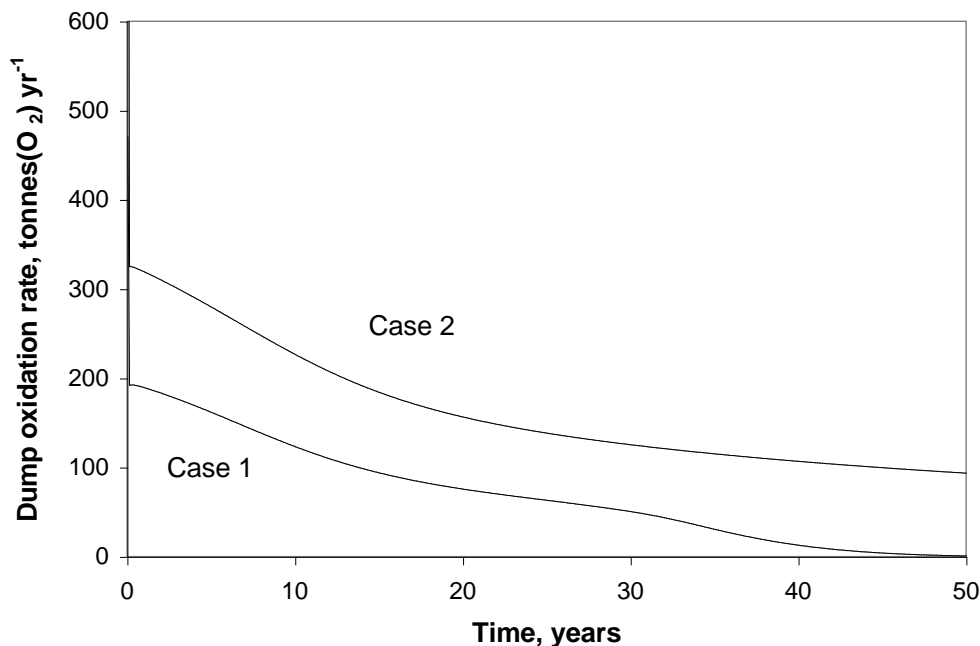


Figure 7. Calculated rate at which the entire dump oxidises, as a function of time (up to 50 years): a comparison of Case 1 (LC PAF dump) and Case 2 (PAF dump).

Figure 8 compares the calculated SO_4^{-2} loads in dump effluent. In both cases there is an initial rapid increase in SO_4^{-2} load. The load reaches a maximum at about 3 years and then slowly decreases. Under the conditions and assumptions used in the model, water residence times in the dumps are of the order of 3 years. It therefore takes up to 3 years for the impact of the near-surface oxidation zone to be reflected in the chemistry of effluent leaving the base of the dump. In the LC PAF dump (Case 1), because reaction ceases within 50 years, the SO_4^{-2} load has dropped to very low levels, ~ 3 tonnes $\text{SO}_4^{-2} \text{ yr}^{-1}$. Loads can be expected to reach their starting levels, < 0.01 tonnes $\text{SO}_4^{-2} \text{ yr}^{-1}$, after a further 3 years, the time it will take to flush all remaining excess sulfate in pore water from the dump.

Calculated Benefits of Cover Emplacement (PAF Material)

Emplacement of covers is a commonly used management strategy to control acid rock drainage from waste rock dumps. Covers are expected to exert control in a number of ways, including by:

- reducing supply of O_2 to reactive sulfide materials and so reducing the generation of acidic products;
- reducing infiltration of water into the dump and so slowing the rate at which water-borne contaminants can be transported through the dump and released from the base. Long

water residence times may lead to higher contaminant concentrations when the water finally reaches the dump base. However, at these higher concentrations, precipitation of secondary minerals within the dump could be another control on contaminant loads and may ensure that loads stay within acceptable limits.

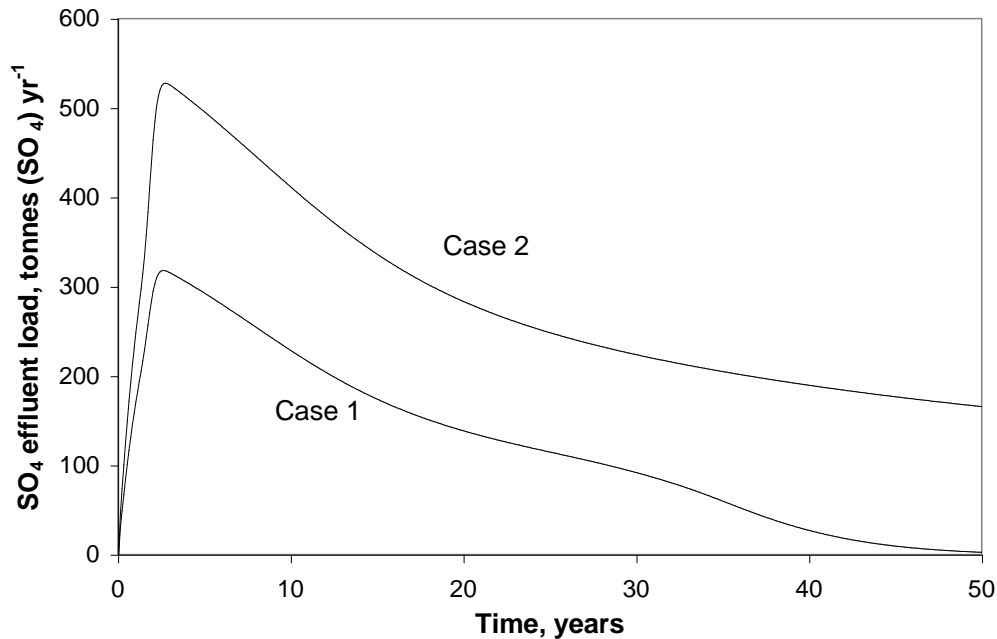


Figure 8. Calculated SO₄ load in dump effluent, as a function of time (up to 50 years): a comparison of Case 1 (LC PAF dump) and Case 2 (PAF dump).

To explore the benefits of cover emplacement for a PAF dump at the Svartliden site, some calculations were undertaken that included the presence of a till cover (see Table 2). Figure 3 showed a schematic of the dump configuration used for simulations. So that the model results could be compared easily with the uncovered dump, the dimensions of the PAF-containing region of the dump remained constant (base-length 50m; height, 10). The dimensions of dump as a whole therefore increased by amounts dependent on the thickness of the emplaced cover (e.g. for a 1m thick cover, the dump base-length is 52m and the height is 11m).

Figure 9 shows the results of calculations involving a high risk PAF dump covered by a layer of glacial till. Emplacement of a glacial till cover is associated with a reduction in the size of the short-term peak in SO₄ load:

- to ~450 tonnes SO₄⁻² yr⁻¹ for the 1m thick cover (a reduction of ~15%);
- to ~300 tonnes SO₄⁻² yr⁻¹ for the 2m thick cover (a reduction of ~43%).

In the longer term, SO₄⁻² loads from the covered dump are slightly higher than those calculated in the case of the uncovered dump.

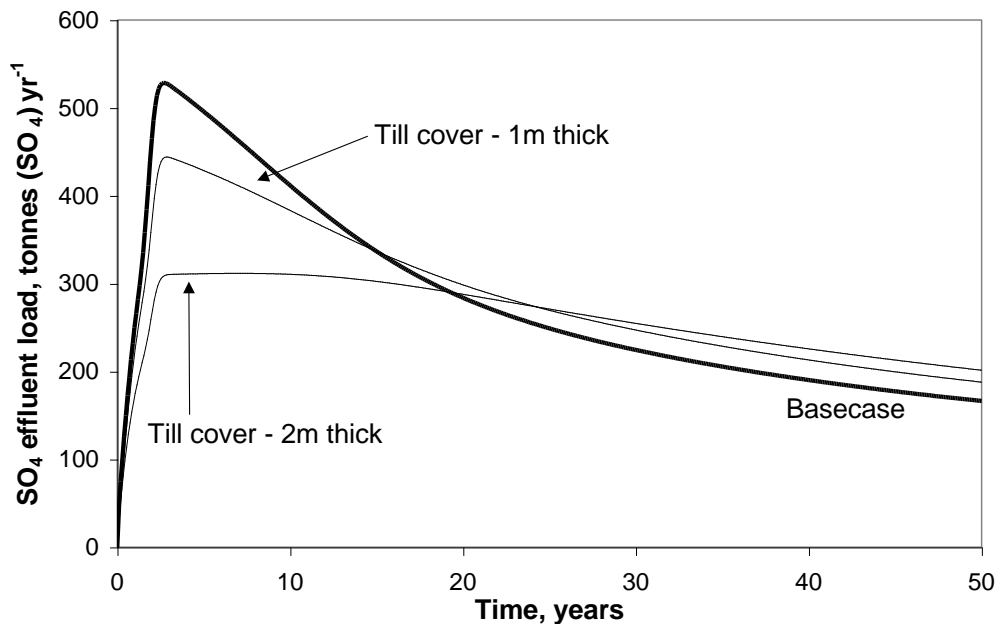


Figure 9. Calculated SO_4^{-2} loads in dump effluent, as a function of time (up to 50 years): The effect of emplacing a cover comprising glacial till, 1m thick or 2m thick. Calculations shown are for Case 2 (high risk PAF dump).

Calculated Behaviour of the Full-Scale Svartliden Dump Design

Figures 10 and 11 illustrate the spatial distribution of oxygen, temperature, and pyrite in the dump at 1 year and 50 years, respectively. The calculation suggest that O_2 will reach the cells eventually, and that oxidation, particularly in the case of the LC PAF cell, will progress significantly over the timescale of interest, 50 years. In fact, by 50 years, most of the sulfide in the LC PAF cell has been consumed (Fig. 11). In the case of the PAF cells, significant pyrite depletion is calculated around the edges of the cells.

Figure 12 compares the SO_4^{-2} load calculated for the model based on the proposed Svartliden design (Case 3), with the combined load expected from two individual dumps, one containing LC PAF (Case1) and the other containing PAF (Case 2). The combined Case 1 + 2 profile shows a single peak in load of ~ 850 tonnes $\text{SO}_4^{-2} \text{ yr}^{-1}$ at just under 3 years, before decreasing relatively steadily over the remainder of the time period studied. The Case 3 load profile shows an initial peak of ~ 940 tonnes $\text{SO}_4^{-2} \text{ yr}^{-1}$ at about 4 years. The slightly higher peak for Case 3 (compared to the Case 1 + 2 profile) is due to the fact that the NAF material surrounding the cells contains some sulfide and is making an additional contribution to the short-term SO_4^{-2} load.

In Case 3, following the short-term peak, the SO_4^{-2} load then decreases before forming a plateau at around 400 tonnes $\text{SO}_4^{-2} \text{ yr}^{-1}$ between 15 and 30 years. After 30 years, the load decreases again. The more complex profile for Case 3 reflects the more complex nature of the dump in question; different regions within the dump commence oxidising at different times. Also, pyrite content varies in the dump and so some dump regions may consume available pyrite more rapidly than others.

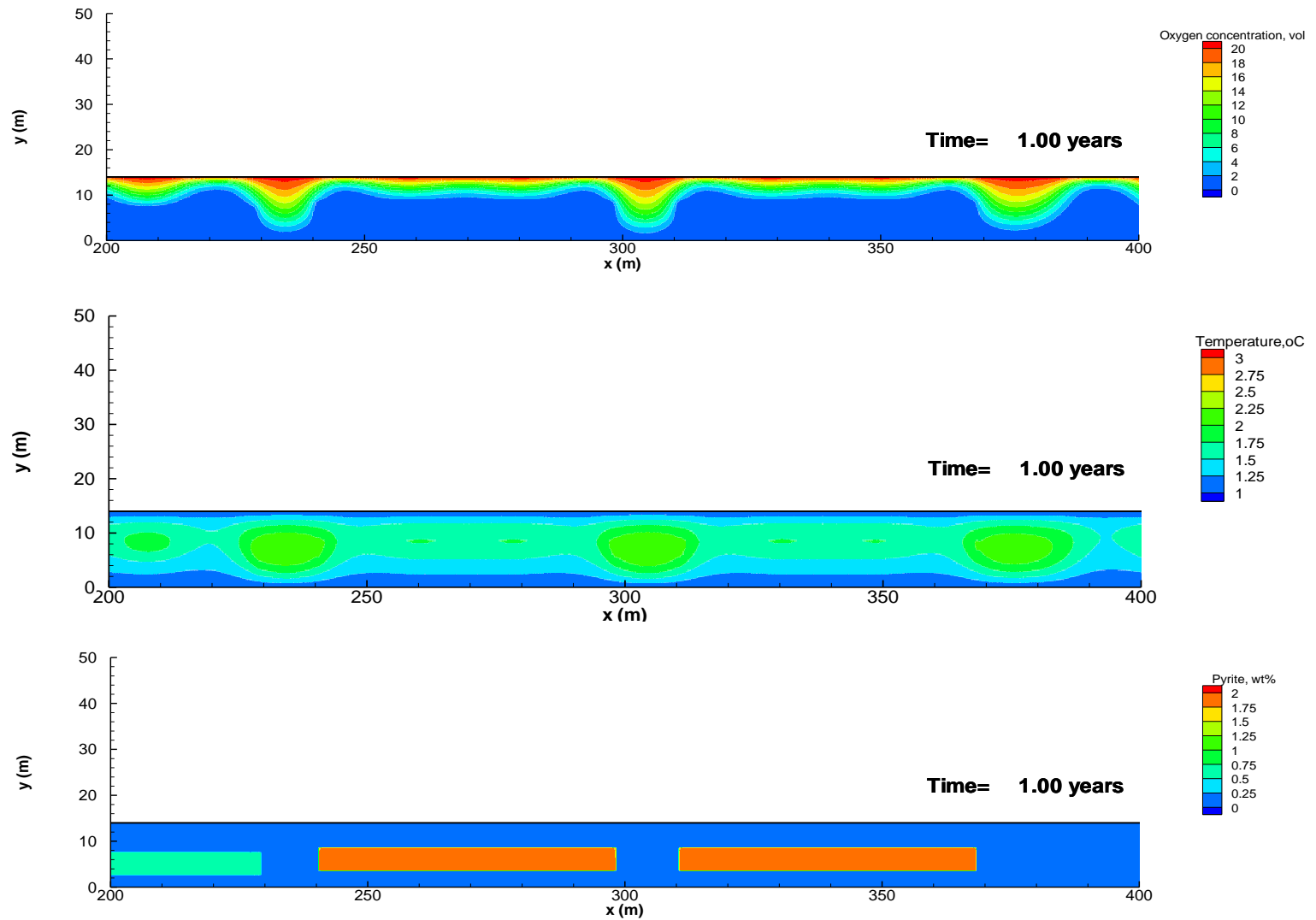


Figure 10. Calculated spatial distribution of O₂, temperature and pyrite at 1 year, Case 3 (full-scale Svartliden dump design). To enable better visualisation of detail, only a portion of the modelled dump is shown, from 200m to 400m (see Fig. 3 for clarification).

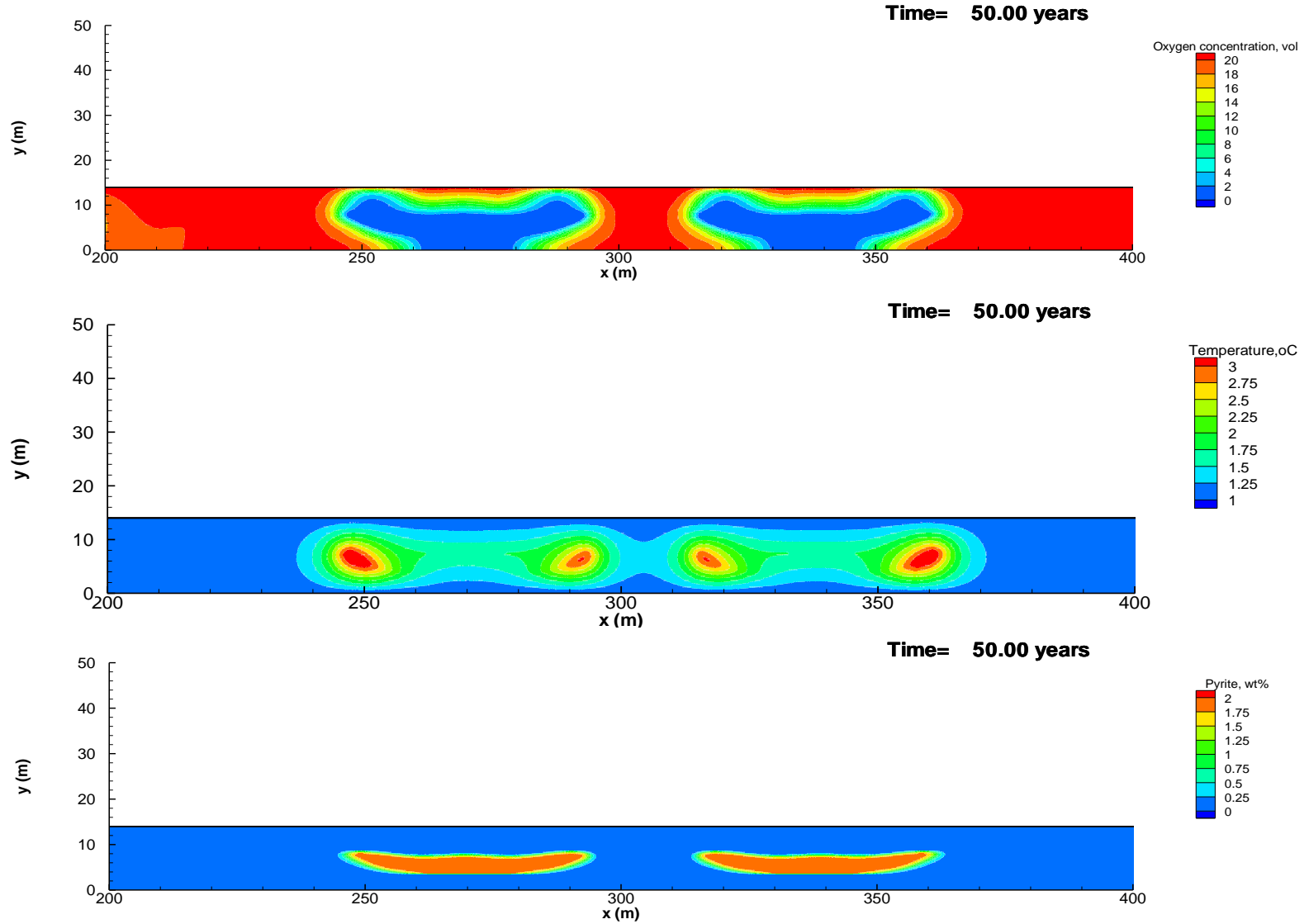


Figure 11. Calculated spatial distribution of O₂, temperature and pyrite at 50 years, Case 3 (full-scale Svartliden dump design). To enable better visualisation of detail, only a portion of the modelled dump is shown, from 200m to 400m (see Fig. 3 for clarification).

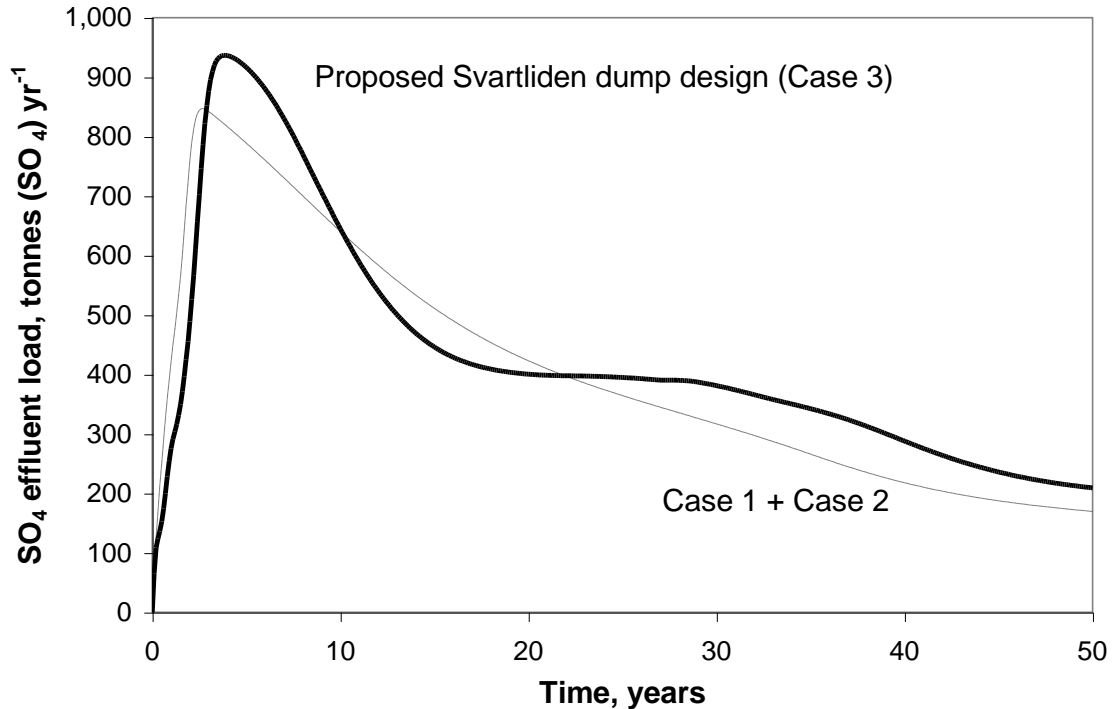


Figure 12. Calculated SO₄⁻² load in dump effluent, as a function of time (up to 50 years): A comparison of Case 3 (based on the planned Svartliden dump design) with the combined load expected from two individual dumps containing LC PAF (Case 1) and PAF (Case2).

Figure 12 suggests that, in terms of total annual SO₄⁻² load expected from the dump(s), the performance of the planned Svartliden design is similar to the combined performance of two individual dumps. However, it is worth noting that the footprint for the planned Svartliden dump is large, 328,000 m². Reactive materials represent less than 14% of the overall dump volume. Thus, per hectare of dump, the Svartliden design will produce a much lower load than would be case for individual dumps. Figure 13 shows the modelled SO₄⁻² load profiles recalculated in terms of annual load per hectare of dump. Judging the benefits of one design over another is complex, and must be undertaken in the context of overall water management at the site. For example, if dump effluent were simply left to seep downwards into the ground underlying the dump, there are clear advantages to reducing the load per hectare of dump. Lower loads imposed over a wide area will impact less on underlying groundwater. The comparison shown in Fig. 13 is therefore of most relevance.

At Svartliden, effluent from the waste rock dump will not be released directly to local water bodies. A dump drainage system has been designed to channel dump seepage towards a nearby sump. If the drainage system is effective, most dump effluent will report to this sump. In this latter scenario, the comparison shown in Fig. 12 is of most relevance. Acidity and contaminant levels associated with the effluent from the different dump scenarios are discussed later in this paper (and will show that although the calculated load profiles are similar, effluent from a dump

based on the Svartliden design is associated with lower contaminant levels than effluent from individual dumps).

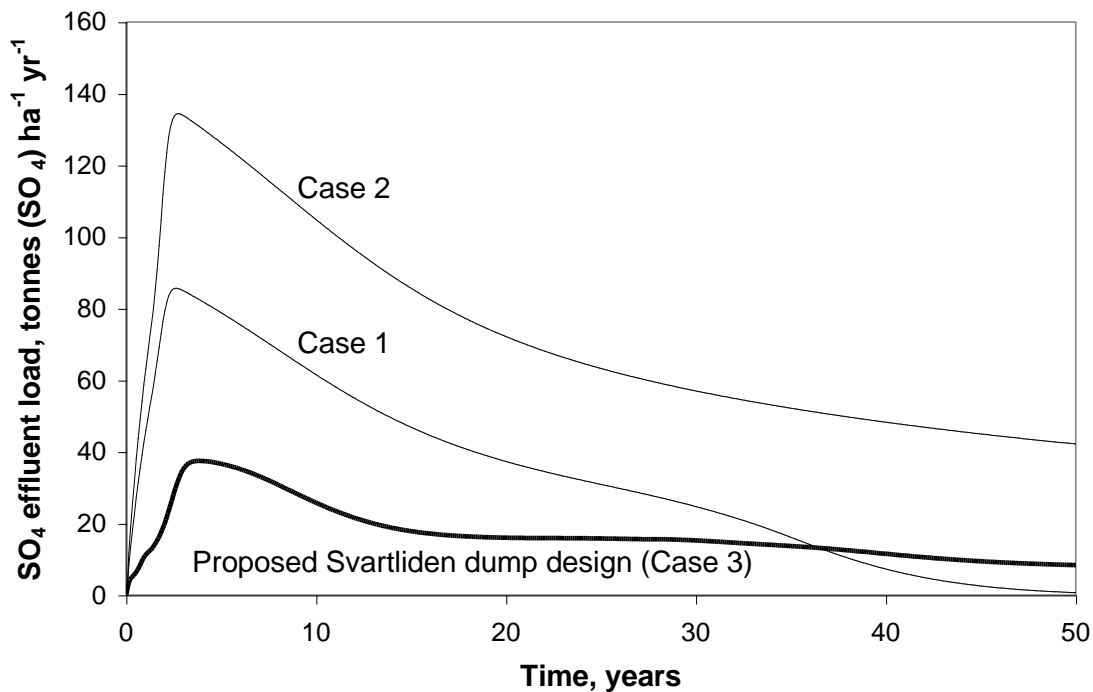


Figure 13. The modelled SO₄⁻² load in dump effluent, recalculated in terms of annual load per hectare, as a function of time (up to 50 years).

Discussion

Sensitivity to Key Input Parameters

To examine the effect that known uncertainties associated with some of the model input parameters might have on model outputs, some additional calculations were undertaken using a range of values for several parameters.

Figure 14 shows the results of calculations where the value selected for the intrinsic oxidation rate (IOR) of the material has been varied (all other parameters remained the same). All three SO₄⁻² load profiles show an initial increase over the first 3 years, corresponding to the time taken for effluent to reflect the oxidation that is taking place in the near-surface of the dump. As expected, the magnitude of the increase is positively correlated with the IOR value. After 3 years, all three profiles decrease, very sharply in the case of the high IOR simulation, moderately sharply for the base-case, and very slowly for the low IOR simulation. The calculated decreases in SO₄⁻² load reflect the fact that (i) pyrite in the dump is being depleted, and (ii) the area oxidising decreases as the oxidation zone moves into the interior of the dump. Pyrite depletion is most rapid in the high IOR case; by ~35 years, pyrite supplies are exhausted, and the SO₄⁻² load reduced to <0.01 tonnes SO₄⁻² yr⁻¹. In the low IOR case, pyrite consumption

is much slower, leading to a SO_4^{-2} profile that never exceeds 100 tonnes $\text{SO}_4^{-2} \text{ yr}^{-1}$, and extends out to times beyond 50 years.

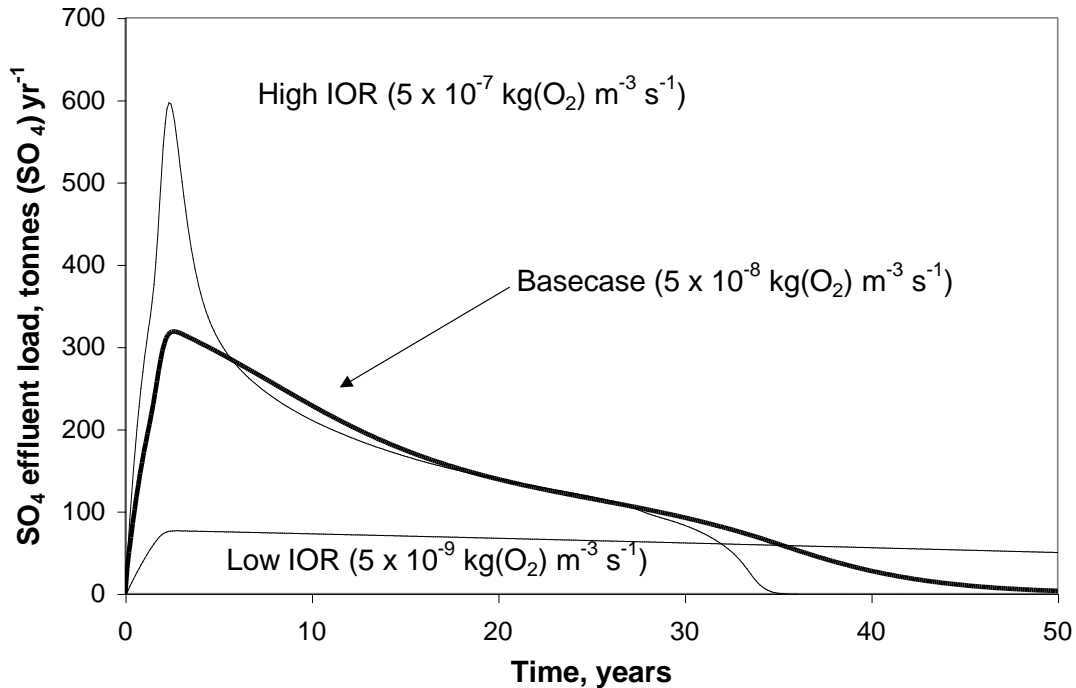


Figure 14. Calculated SO_4^{-2} load in dump effluent, as a function of time (up to 50 years): The effect of uncertainty in IOR on model output. Calculations shown are for Case 1 (LC PAF dump).

Figure 15 shows the results of calculations where the value selected for the dump water infiltration rate has been varied (all other parameters remained the same). Three values were selected:

- base-case – 0.446 m yr^{-1} (see Table 1);
- high infiltration rate – 2.436 m yr^{-1} . This rate equates to a situation where the maximum measured monthly rainfall (203mm) is maintained all year and there is no significant evaporation. It further assumes that all this rain infiltrates the dump. This is an ‘extreme’ case for the Svartliden site conditions;
- low infiltration rate – the base-case value divided by 10. Data for the Svartliden site suggests that, in some months, a combination of low rainfall and high evaporation could lead to zero infiltration to the dump. For the current study, the selected value, 0.04 m yr^{-1} , corresponds to a monthly infiltration of $\sim 3\text{mm}$, i.e. a low, but non-zero, extreme.

Changing the infiltration rate also changes the water residence time in the dump and also the water content in the dump (which in turn affects gas-filled porosity and effective diffusion of gas in the dump).

The main differences seen in the SO_4^{-2} load profiles shown in Fig. 15 relate to water residence time. Longer residence times result in longer elapsed times before the profile reaches peak SO_4^{-2} load: <1 year for the high infiltration rate, 3 years for the base-case, and just under 20 years for the low infiltration rate.

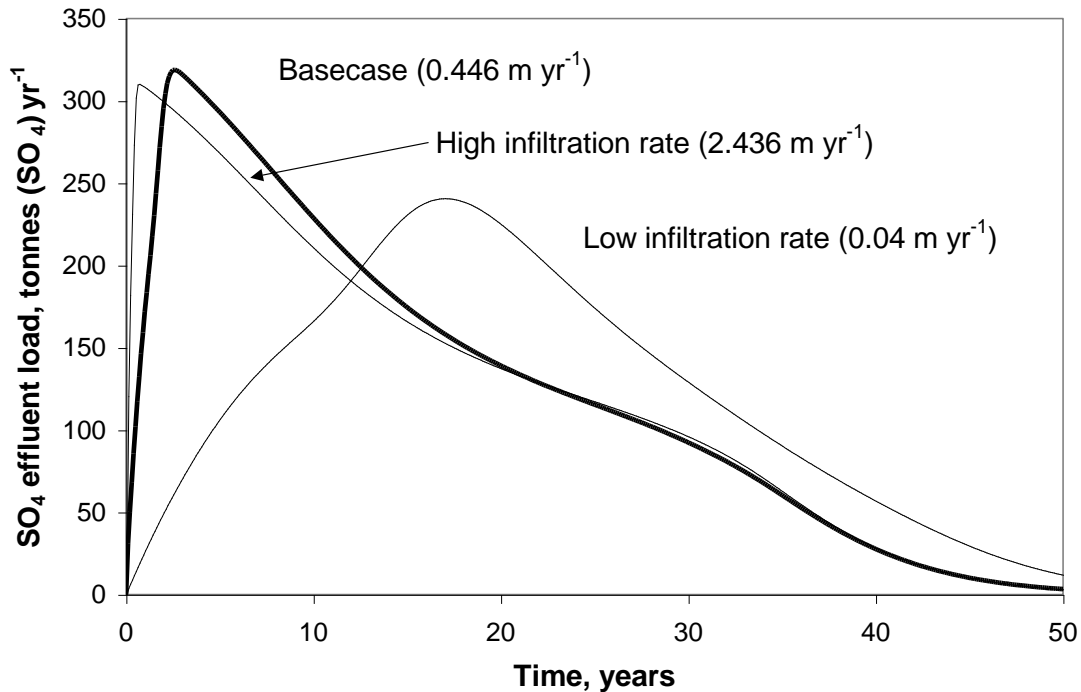


Figure 15. Calculated SO_4^{-2} load in dump effluent, as a function of time (up to 50 years): The effect of uncertainty in water infiltration rate on model output. Calculations shown are for Case 1 (LC PAF dump).

Important controls on O_2 transport in the dump are the gas-filled porosity (which affects the effective O_2 diffusion coefficient, D_e) and the gas permeability. The former property governs diffusive transport and the latter governs advection. To examine the sensitivity of the system to gas transport properties of the waste rock the following calculations were undertaken:

- base-case – gas permeability, 10^{-10} m^2 ; gas-filled porosity, 0.20 (giving a calculated D_e , $2.5 \times 10^{-6} \text{ m}^2 \text{ s}^{-1}$);
- slow gas transport – gas permeability, 10^{-11} m^2 ; gas-filled porosity, 0.115 (giving a calculated D_e , $1.4 \times 10^{-6} \text{ m}^2 \text{ s}^{-1}$);
- rapid gas transport - gas permeability, 10^{-8} m^2 ; gas-filled porosity, 0.28 (giving a calculated D_e , $3.5 \times 10^{-6} \text{ m}^2 \text{ s}^{-1}$).

Figure 16 shows the results of these calculations. The calculated SO_4^{-2} load profiles are very different. In the case of rapid gas transport, a greater proportion of the heap is oxygenated leading to rapid overall dump oxidation rates. There is a high peak SO_4^{-2} load (~770 tonnes $\text{SO}_4^{-2} \text{ yr}^{-1}$) after a very short time (around 6 months). However, pyrite is consumed

rapidly and by 25 years the SO_4^{-2} load has dropped back to initial levels of <0.01 tonnes SO_4^{-2} yr^{-1} . In contrast, in the case of slow gas transport, the peak load is much lower (~ 135 tonnes SO_4^{-2} yr^{-1}) and is reached after a longer elapsed time (5 years).

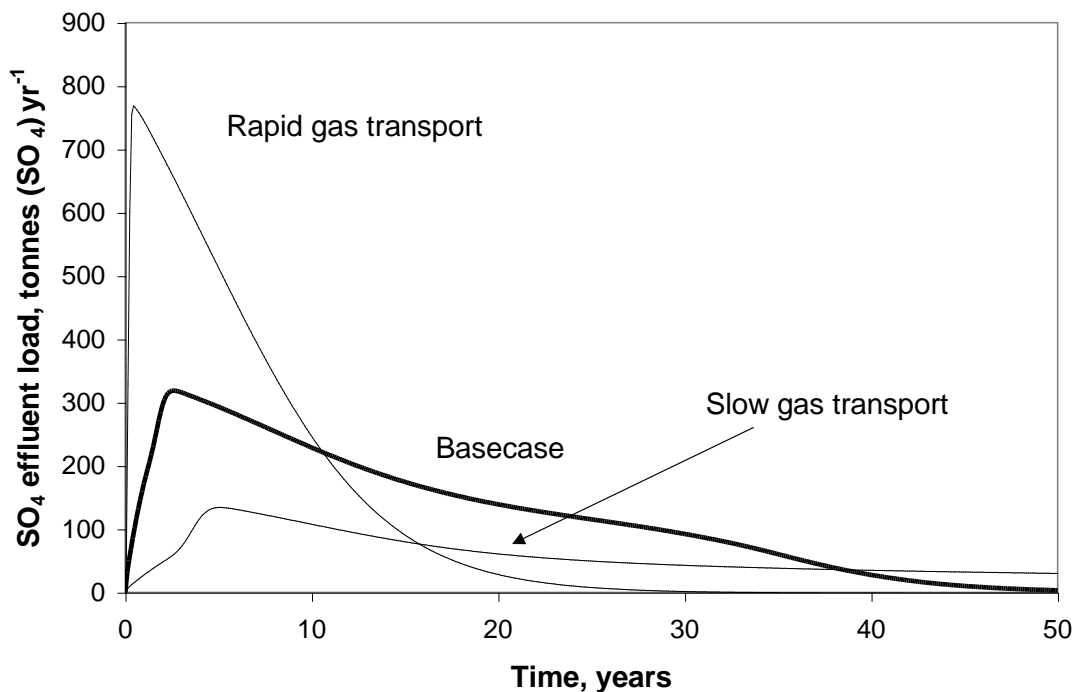


Figure 16. Calculated SO_4^{-2} load in dump effluent, as a function of time (up to 50 years): The effect of uncertainty in gas transport properties on model output. Calculations shown are for Case 1 (LC PAF dump).

These sensitivity calculations have given an indication of how parameter uncertainty might affect the predicted load profiles. In many cases, the overall effect is to reduce the magnitude of the initial peak in load and spread the profile out over a longer timescale. The key exceptions are unexpectedly high IOR values and/or very permeable dump materials. In these latter cases, the initial loads could be significantly higher than expected. However, the load profiles will ‘decay’ more rapidly and at longer elapsed times, the loads will be lower.

Acidity and contaminant levels in dump effluent

The planned dump footprint at Svartliden is $328,000 \text{ m}^2$. Based on a water infiltration rate of 0.446 m yr^{-1} (the base-case value used in the current work), the annual discharge from the dump will be of order $1.5 \times 10^5 \text{ m}^3$. Based on Fig. 12, the peak SO_4^{-2} load expected from the planned Svartliden design (Case 3) is ~ 940 tonnes yr^{-1} . The corresponding SO_4^{-2} concentration is 6.4 g L^{-1} . According to Fig. 12, this peak is short lived, and over most of the profile, loads are less than 400 tonnes SO_4^{-2} yr^{-1} , corresponding to SO_4^{-2} concentrations less than 3 g L^{-1} .

The combined footprint of the Case 1 and Case 2 dumps (individual dumps containing LC PAF and PAF, respectively) is $76,400 \text{ m}^2$. The annual discharge from the dumps would be $3.4 \times 10^4 \text{ m}^3$. For the combined dumps, the peak SO_4^{-2} load was 850 tonnes yr^{-1} (Fig. 12),

corresponding to a SO_4^{-2} concentration of 25 g L^{-1} , a factor of 4 higher than was the case for the planned Svartliden design.

In Sweden, no regulatory limits have been imposed with respect to SO_4^{-2} . According to the World Health Organisation guidelines (2004), there are no health concerns related to sulfate, although it is noted that levels in excess of 1 g L^{-1} may adversely affect the taste of drinking water (e.g. typical seawater contains 2 to $3 \text{ g L}^{-1} \text{ SO}_4^{-2}$ Appelo and Postma, 1994).

Modelled Fe and H loads have not been presented in this paper as they show trends equivalent to the calculated SO_4^{-2} loads. Aqueous speciation, neutralisation and mineral precipitation are neglected in the current study. Such processes are expected to exert a strong influence on Fe and H behaviour. For example, mineral precipitation often controls Fe levels in dump pore water and often leads to low Fe concentrations in contacting water. It is hoped that future work might include a more detailed representation of the geochemistry of the dump. For an example of SULFIDOX calculations that include full geochemistry, the reader is referred to Linklater et al, 2005.

Summary

An improved version of the SULFIDOX modelling code has been used to quantify the benefits of the complex dump design proposed for the Svartliden site. The calculations have shown that

- including a low-permeability cover or lining within the dump design can reduce initial peaks in SO_4^{-2} loads; a 1m thick cover resulted in a 15% reduction, whereas a 2m thick cover resulted in a 43% reduction;
- in terms of total annual SO_4^{-2} load expected from the dump(s), the performance of the planned Svartliden design is similar to the combined performance of two individual dumps;
- in terms of load per hectare of dump, the Svartliden design will produce a lower load than would be case for individual dumps (up to a factor of 4);
- in terms of contaminant concentrations in the dump effluent (using SO_4^{-2} as an indicator), the Svartliden design is associated with significant reductions (around a factor of 4 to 5).

Most of the calculated benefits arise through control of the supply of oxygen to highly reactive materials (i.e. the lining of low-permeability till around the PAF wastes), and by controlling the volume of the overall dump occupied by reactive materials. Judging the benefits of one dump design over another is complex, and must be undertaken in the context of overall water management at the site.

Acknowledgements

Joshua Stewart (Dragon Mining NL) prepared the dump designs that form the basis of this work. Dr Anders Brundin (Dragon Mining NL) is acknowledged for assistance with regulatory aspects. Interpretation of data and model outputs benefited greatly from discussions with Andrew Garvie (ANSTO Minerals).

Literature Cited

- Appelo, C.A.J. and Postma, D. 1994. *Geochemistry, groundwater and pollution*. Published by Balkema, Rotterdam.
- Bennett, J.W., Ritchie, A.I.M. and Tan, Y. 1993. The temperature dependence of pyritic oxidation rates in waste rock at the Aitik mine. ANSTO Technical Report ANSTO/C335.
- Bennett J.W., Comarmond, M.J., and Jeffery, J.J. 2000. Comparison of sulfidic oxidation rates measured in the laboratory and the field. In: *Proceedings of the Fifth International Conference on Acid Rock Drainage, ICARD 2000*. 21-24 May 2000. Denver, Colorado. Vol.1, pp.171-180.
- Brown, P.L. and Comarmond, M.J. 2003. Neutralisation of acidity generated by the oxidation of sulfide minerals at the Svartliden mine. ANSTO Technical Report, ANSTO/C727.
- Brown, P.L., Crawford, J., Irannejad, P., Miskelly, P.C., Noël, M.M., Pantelis, G., Plotnikoff, W.W., Sinclair, D.J. and Stepanyants, Y.A. 2001. SULFIDOX: Version 1.1. A tool for modelling the temporal and spatial behaviour of heaps containing sulfidic minerals. ANSTO Technical Report, ANSTO/ED/TN01-03.
- Brown, P.L., Haworth, A., Sharland, S.M. and Tweed, C.J. 1991. HARPHRQ: A geochemical speciation program based on PHREEQE. Nirex Report NSS/R379.
- Comarmond, M.J. and Brown, P.L. 2002. Geochemical characterisation of RC material, Svartliden Gold Project, Dragon Mining NL. ANSTO Technical Report, ANSTO/C718.
- Comarmond, M.J., Brown, P.L. and Innes, E.Q. 2003. Column studies, Svartliden Gold Project, Dragon Mining NL. ANSTO Technical Report, ANSTO/C723.
- Hammack, R.W. and Watzlaf, G.R. 1990. The effect of oxygen on pyrite oxidation. In: *Proceedings of the Mining and Reclamation Conference, Charleston, WV, April 23-26*, pp.257-264. <https://doi.org/10.21000/JASMR90010257>
- Linklater, C.M., Sinclair, D.J. and Brown, P.L. 2005. Coupled chemistry and transport modelling of sulphidic waste rock dumps at the Aitik mine site, Sweden. *Applied Geochemistry*, 20, 275-293. <http://dx.doi.org/10.1016/j.apgeochem.2004.08.003>.
- Nicholson, R.V. 1994. Iron-sulfide oxidation mechanisms: Laboratory studies. *In: (Jambor, J.L. and Blowes, D.W (Eds). The Environmental Geochemistry of Sulfide Mine-Wastes. Min. Soc. Canada Short Course Handbook Volume 22.*
- Pantelis, G., Ritchie, A.I.M. and Stepanyants, Y.A. 2002. A conceptual model for the description of oxidation and transport processes in sulphidic waste dumps. *Appl. Math. Modelling*, 26, 751-770. [http://dx.doi.org/10.1016/S0307-904X\(01\)00085-3](http://dx.doi.org/10.1016/S0307-904X(01)00085-3).
- Parkhurst, D.L., Thorstenson, D.C. and Plummer, L.N. 1980. PHREEQE – A computer program for geochemical calculations, U.S. Geological Survey, Water Resources Investigations Report 80-96.
- Ritchie, A.I.M. 1994. Sulfide oxidation mechanisms: Controls and rates of oxygen transport. *In: (Jambor, J.L. and Blowes, D.W (Eds). The Environmental Geochemistry of Sulfide Mine-Wastes. Min. Soc. Canada Short Course Handbook Volume 22.*

World Health Organisation, 2004. Guidelines for Drinking-Water Quality, 3rd Edition, Volume 1: Recommendations.